공학석사 학위논문

Characteristics of Pt-BaO/Hydrotalcite Catalysts for NOx Storage-Reduction Reaction

질소 산화물 흡장 환원 반응에서 하이드로탈사이트에 담지된 Pt-BaO 촉매의 특성

2013년 8월

서울대학교 대학원

화학생물공학부

정 소 연

Abstract

Characteristics of Pt-BaO/Hydrotalcite Catalysts for NOx Storage-Reduction Reaction

Soyeon Jeong
Master's Program
School of Chemical and Biological Engineering
Seoul National University

Diesel engines are operated under excess of oxygen, so conventional three-way catalyst hardly removes NOx emitted from diesel engines. To remove NOx more effectively, NOx Storage Reduction (NSR) technology is being used as one of the potential methods. The typical NSR catalyst, Pt-BaO/Al_2O_3, shows good performance; however, there are drawbacks such as inferior thermal stability and narrow active temperature region. This study

addresses the use of Mg-Al mixed oxide, known as hydrotalcite material as NSR catalyst support to overcome these disadvantages. In this work, hydrotalcite was synthesized with various Mg/Al molar ratios and used NSR catalyst support on which Pt and Ba were loaded.

Hydrotalcite (HT) was prepared by applying co-precipitation method with the Mg/Al ratios of 1:9, 2:8, 3:7, 4:6, 5:5 and 6:4. Hydrotalcite was then calcined at 800 ℃ and used as NSR catalyst support. All prepared catalysts were calcined at 500 ℃, 650 ℃ and 800 ℃, and the NOx storage activity of the catalysts was examined. Then, various characterizations were performed by the means of BET specific surface area, XRD, ICP, FT-IR, CO chemisorption, TEM/ EDS and NO_2-TPD.

On the samples calcined at 500 ℃, the NOx storage activities of HT-supported catalysts were superior to that of Al_2O_3 supported one. Also, the range of active temperature region was shifted to high temperature while that of Pt-BaO/Al_2O_3 catalyst was narrow. Especially, for the case of sample with the Mg/Al ratio of 2:8, the temperature where the activity is maximized is 400 ℃. On the samples calcined at higher temperature (650 ℃ and 800 ℃), the activity of Pt-BaO/Al_2O_3 catalyst was completely deactivated in all temperature regions due to the sintering of Pt while HT-supported catalysts still show remarkable NOx storage ability especially in high

temperature region. It was confirmed that catalysts supported on Mg-Al mixed oxide have better thermal durability such as activity, minimized Pt sintering and less $BaAl_2O_4$ formation, thus better NOx storage activity. Especially, Mg/Al ratio is 4:6.

This study provides the information on optimal Mg/Al ratio to use hydrotalcite as support for NSR reaction. When Pt and Ba were loaded on the support, HT-supported catalysts showed superior NOx storage performance compared with Al_2O_3-supported catalyst even after high temperature treatment. Also, we confirmed the positive effect of MgO on the stability of Pt. In summary, it was found that the use of hydrotalcite as NSR catalyst support can aid in improving NOx storage activity and Pt dispersion, and inhibiting sintering of Pt, thus potentially substituting Al_2O_3 support.

Keywords: NOx Storage Reduction, Hydrotalcite, Mg/Al ratio, Pt-BaO, Thermal durability

Student Number: 2011-23414

Contents

List of Tables

List of Figures

Chapter 1. Introduction

1.1. Background of diesel engines and their emission regulations

Diesel engines have better fuel economy and more power than gasoline engines. These facts are good enough to attract users [1]. Also, costs to maintain diesel engines are reasonable, and diesel engines emit low exhaust gases, such as CO and hydrocarbon (HC) [2-4]. A diesel engine is always operated under excess of oxygen. Because of this reason, CO and hydrocarbon (HC) can be easily oxidized and emit lower exhaust gases. However, this system makes control of NOx emissions difficult because NOx cannot be converted without a reductant [5-7]. Another disadvantage of diesel engines is emission of particulate matters that consist mostly of carbonaceous soot and soluble organic fraction (SOF) of hydrocarbons. As mentioned above briefly, diesel engines emit various air pollutants such as HCs, CO, NOx along with particulates, and those pollutants lead to serious environment problems. Actually, there is the fact that anthropogenic emissions of NOx in Europe contribute to about 30 % of global NOx emissions in 1990, and transports (diesel vehicles) account for about 30-50 %

in the figure [8].

Emission standards in Europe have been divided in several categories as shown in Table 1. Compared to early 1990s, emission regulation of NOx is getting more stringent for gasoline PCs, LDVS, and Diesel things [6, 8]. A situation on NOx control in North America is also similar with Europe. As shown in Figure 1, US Bin 2 and CA SULEV II are almost one tenth of US Bin 10 [2]. Through this information, the fact that several efforts have to be made to meet strict NOx emission regulations is obvious. NOx emission standards have been met by only engine control measures so far; however, it is hard to meet the regulation only with conventional means for the future, so lean NOx control techniques for more efficient NOx removal have been developed [4, 7].

Table 1. Emission standards for road transport in Europe post-1992 [8]

Emission Standard	Regulation	Impl. Year[1]	NO_x (g/km) or (g/kWh)	NO_x (Gg/PJ) [Converted]	Main technology improvements over preceding step
Gasoline PCs and LDVs (g/km)					
Euro 1	91/441/EC	1992	0.62[2]	0.25	Closed-loop TWC[3]
Euro 2	94/12/EC	1996	0.35[2]	0.14	Faster light-off
Euro 3	98/69/EC	2000	0.15	0.06	Faster light-off and twin lambda control
Euro 4	98/69/EC	2005	0.08	0.03	Faster light-off and improved lambda control
Euro 5 and 6	EC 715/2007	2010–2015	0.06	0.02	Improved aftertreatment materials, deNOx for direct injection vehicles
Diesel PCs and LDVs (g/km)					
Euro 1	91/441/EC	1992	0.90[2]	0.44	Improved combustion
Euro 2	94/12/EC	1996	0.67[2]	0.32	Oxidation catalyst
Euro 3	98/69/EC	2000	0.50	0.24	Two oxidation catalysts, high pressure injection
Euro 4	98/69/EC	2005	0.25	0.12	Precise injection and pressure control
Euro 5	EC 715/2007	2010	0.18	0.09	Diesel particle filters
Euro 6	EC 715/2007	2010	0.08	0.04	deNOx, presumably SCR[3]
HDVs (g/kWh)					
Euro I	91/542/EEC	1992	8.0	0.84	Improved combustion
Euro II	91/542/EEC	1996	7.0	0.74	Electronic engine control
Euro III	1999/96/EC	2000	5.0	0.56	High pressure injection
Euro IV	1999/96/EC	2005	3.5	0.40	EGR, precise injection control
Euro V	1999/96/EC	2008	2.0	0.25	Cooled EGR[3] or SCR
Euro VI	Only draft proposal	2014	0.4	0.05	Presumably SCR+DPF[3]

[1] For LDVs and HDVs. For LDVs, the implementation date is roughly one year later than PCs to allow for calibration of new technology.
[2] Regulations set a standard for the sum of HC and NO_x emissions. The value quoted in the table is an inferred value based on typical HC/NO_x split for the particular vehicle technology.
[3] TWC: Three-way catalytic converter; SCR: Selective catalytic reduction; DPF: Diesel particle filter.

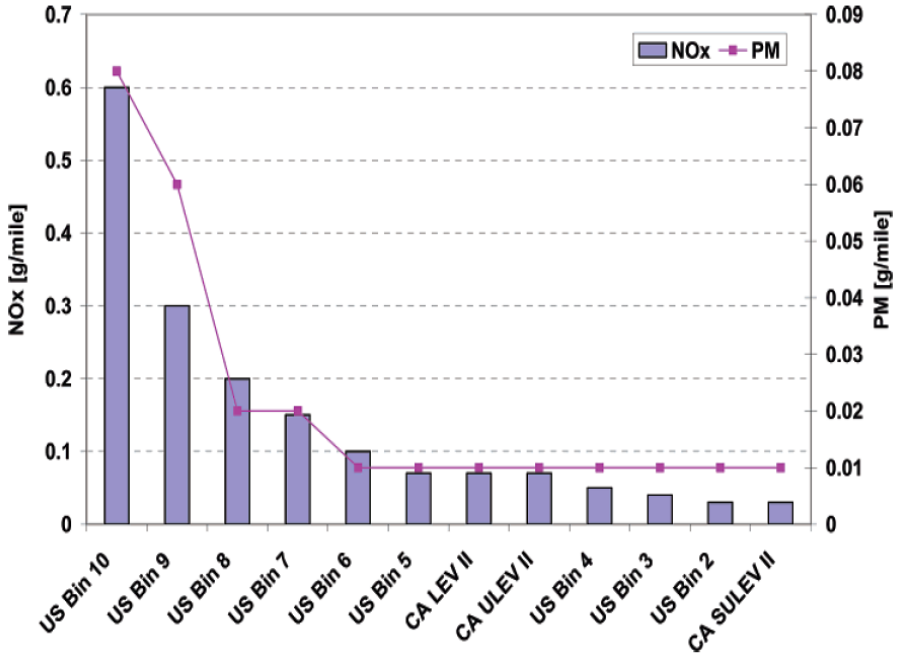

Figure 1. North American NOx and Particulate matter regulation (Note : Bins 9 and 10 are fully phased-out after the 2008 model year) [2].

1.2. Background of Hydrotalcites (HTs)

The general terms of hydrotalcite-like compounds are layered double hydroxides (LDH's) and anionic clay minerals. The general formula for description of the chemical composition is $[M_{1-x}^{z+}M_x^{3+}(OH)_2]^{b+}[A_{\frac{b}{n}}^{n-}]\mathrm{m}H_2\mathrm{O}$, where M=metal, A=interlayer anion, and b=x or 2x-1 for z=2 or 1, respectively [9-11]. Among the various types of hydrotalcites, discovered in Sweden around 1842, $Mg_6Al_2(OH)_{16}(CO_3)\cdot 4H_2O$ form has been broadly investigated [11, 12]. This type consists of brucite and cation layers of magnesium and aluminum hydroxide octahedral sharing edges. Also, there are carbonate anions and water molecules between the metal hydroxide layers as indicated Figure 2 [10, 13]. Hydrotalcites have been used mainly after calcination because several attractive properties are induced by calcining hydrotalcites. (1) high surface area (100-300 m^2/g), (2) basic properties, (3) formation of homogeneous mixed oxide with thermal stability, and (4) memory effect, reconstruction original hydrotalcite structure under mild conditions [14]. Due to these advantages, hydrotalcite has found many practical applications such as catalysts, catalyst supports, industry, medicine, and adsorbents [10, 14]. More detailed applications of

HTs are shown in Figure 3 [11].

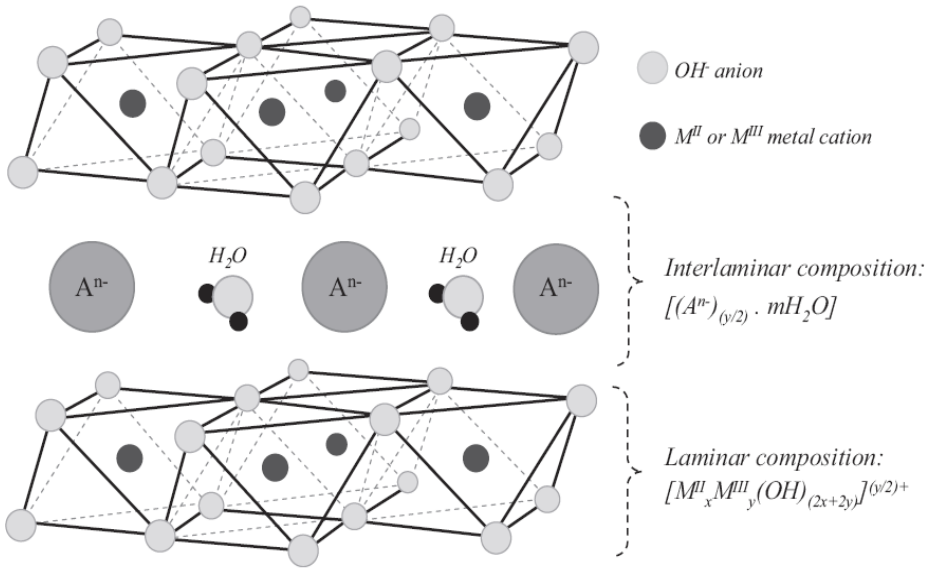

Figure 2. Schematic representation of the hydrotalcite structure [11].

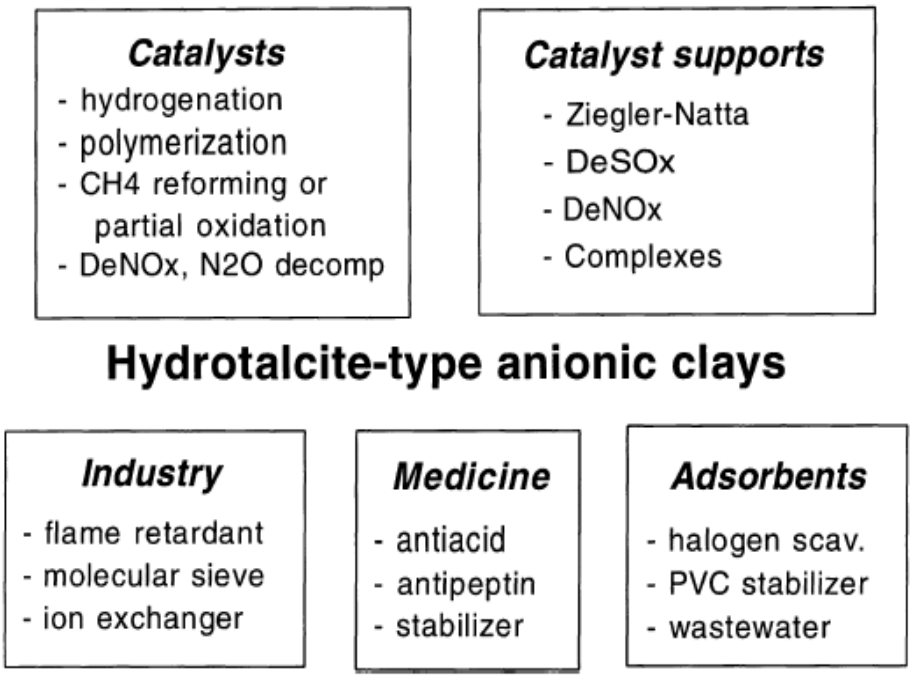

Figure 3. Main industrial applications of anionic clays (as such or after thermal decomposition) [10].

1.3. Objective

NOx emissions from diesel engines operated under lean conditions are rarely reduced with conventional three-way catalysts [15]. An alternative to overcome this weakness is NOx storage-reduction (NSR) catalyst system. NSR catalyst has gained attraction to be efficient methods for aftertreatment techniques of diesel engines, which operate under excess of oxygen, and Pt-BaO/Al_2O_3 catalysts are conventionally used in NSR systems [16-20]. However, storage performances in Pt-BaO/Al_2O_3 easily deteriorate due to incomplete reduction of bulk barium nitrates in rich condition and formation of $BaAl_2O_4$ or $BaPtO_3$ that would interrupt storage performances at high temperature [16]. HT-supported catalysts have been studied to improve NSR performance because of their several advantages such as their high surface areas and structural stability [10, 14, 15, 18]. Even though there are many cases on HTs in NSR catalyst systems, researches that mention the effect of HTs synthesized by changing molar ratio of magnesium and aluminum are insufficient. In this study, Pt-BaO/HTs were developed and investigated for NSR systems. Hydrotalcites were synthesized with various molar ratios of magnesium and aluminum. Also, the conventional NSR catalyst, Pt-BaO/Al_2O_3, was compared with HT-supported catalysts in NSR systems.

Chapter 2. Theoretical formulation

2.1. Diesel engines aftertreatment systems

Diesel engines emit low concentration of CO_2, and their fuel efficiency is reasonable. However, development of a new aftertreatment system for diesel engines is necessary because the conventional three-way catalysts are inefficient to remove NOx from diesel engines under excess of oxygen. Thus, the aftertreatreatment system of diesel engines is more complicated than gasoline engines [21, 22]. There are three major aftertreatment techniques of diesel exhaust systems:

(1) DOC (Diesel Oxidation Catalyst)

(2) SCR (Selective Catalytic Reduction)

(3) NSR (NOx Storage Reduction)

2.1.1. Diesel Oxidation Catalyst (DOC)

Exhaust gas from diesel engines consists of gaseous, liquid, and solid components, and the three-way catalysts (TWC) used for gasoline engines are insufficient to be used in diesel engines because TWC is operated under lower

air to fuel ratio condition (14.6) than that of diesel engines. Condition of excess of oxygen makes the reduction of NOx more difficult [23]. Diesel oxidation catalysts (DOCs) are one of the aftertreatment systems of diesel engines which can oxidize CO and hydrocarbons and remove particulate matter (PM) [24, 25]. Control of both NOx and particulate matter (PM) emission is difficult at the low temperatures of diesel emission because once one is controlled at low temperature, then the other is hardly controlled. DOCs with noble metals, such as Pt and Pd, offer good oxidation performance for CO, hydrocarbon, and soluble organic fraction (SOF) components; SOF oxidation leads to reduction of PM as well [26]. However, these catalysts are not good in another way because SO_2 oxidation reaction occurs [23, 27]. Oxidized SO_2 may produce SO_3 and H_2SO_4 formed by reacting with H_2O. Although DOCs are very efficient to reduce emissions of CO, hydrocarbons, and PM, there is still drawback that leads to formation of SO_3 and H_2SO_4, so improvement for the technique to meet getting more stringent environment regulations is inevitable [27].

2.1.2. Selective Catalytic Reduction (SCR)

A study for NOx reduction has become a great challenge to meet

environment regulations. Many catalysts are used to eliminate NO with various ways;

1. Selective catalytic reduction of NO with ammonia
2. Catalytic reduction of NO in the present of CO
3. Selective catalytic reduction of NO in the presence for hydrocarbons
4. Catalytic reduction of NO with hydrogen

Especially, the selective catalytic reduction with ammonia, known as NH_3-SCR, is broadly used in many industries to control NOx emissions. This reaction formula is indicated below. As indicated in the equations below, an ammonia molecule reacts to a NO molecule, and two ammonia molecules are needed to react to one NO_2 molecule.

$$4NH_3 + 4NO + O_2 \rightarrow 4N_2 + 6H_2O$$

$$4NH_3 + 2NO_2 + O_2 \rightarrow 3N_2 + 6H_2O$$

NH_3-SCR is not proper for mobile applications because its weaknesses such as odor, leakage, and supply problem exist. Due to these disadvantages, another alternative is suggested, that is urea-SCR. Urea is cost-effective and easy to use. However, urea system also has problems which are difficult to be decomposed and can produce byproducts. These issues interrupt the use of urea/NH_3-SCR for mobile applications [27-30].

Nowadays, use of hydrocarbons as a reductant in SCR is one of the

most prospective ways to remove NO [28]. HC-SCR has an advantage which uses a gas mixture, but that may lead to low fuel efficiency and increase CO emissions [27]. To improve these problems, various types of researches are in progress.

2.1.3. NOx Storage Reduction (NSR)

A promising alternative for NOx removal under lean conditions is NOx storage-reduction (NSR) system [7, 22, 31]. The system has been addressed at first by Toyota researchers and suggests the possibility to control NOx emission from diesel engines even under excess of oxygen condition [32, 33].

Conventional NSR catalysts consist of support, NOx storage components (e.g. an alkaline or alkaline-earth metal oxide) such as Ba, Mg, K, or Na, and noble metal such as Pt [32, 34, 35]. A NOx storage component is for storing oxidized NO_2, and a noble metal is to oxidize NOx. NSR catalytic systems, also referred to as lean NOx traps (LNTs), are operated under both lean and rich conditions. During a lean cycle, NOx is oxidized by Pt, and oxidized NO_2 is stored on Ba sites as nitrate forms. Also, in a rich cycle, stored nitrate forms are reduced as N_2, CO_2, and H_2O by various

reductants such as H_2, CO, and/or hydrocarbons [33, 35]. Figure 4 shows mechanism of NSR reaction system well.

Typically used catalyst for NSR system is Pt-BaO/Al_2O_3. This catalyst shows good performance on NSR reaction, but it can be easily poisoned by sulfur, so more development on this is needed [32, 34].

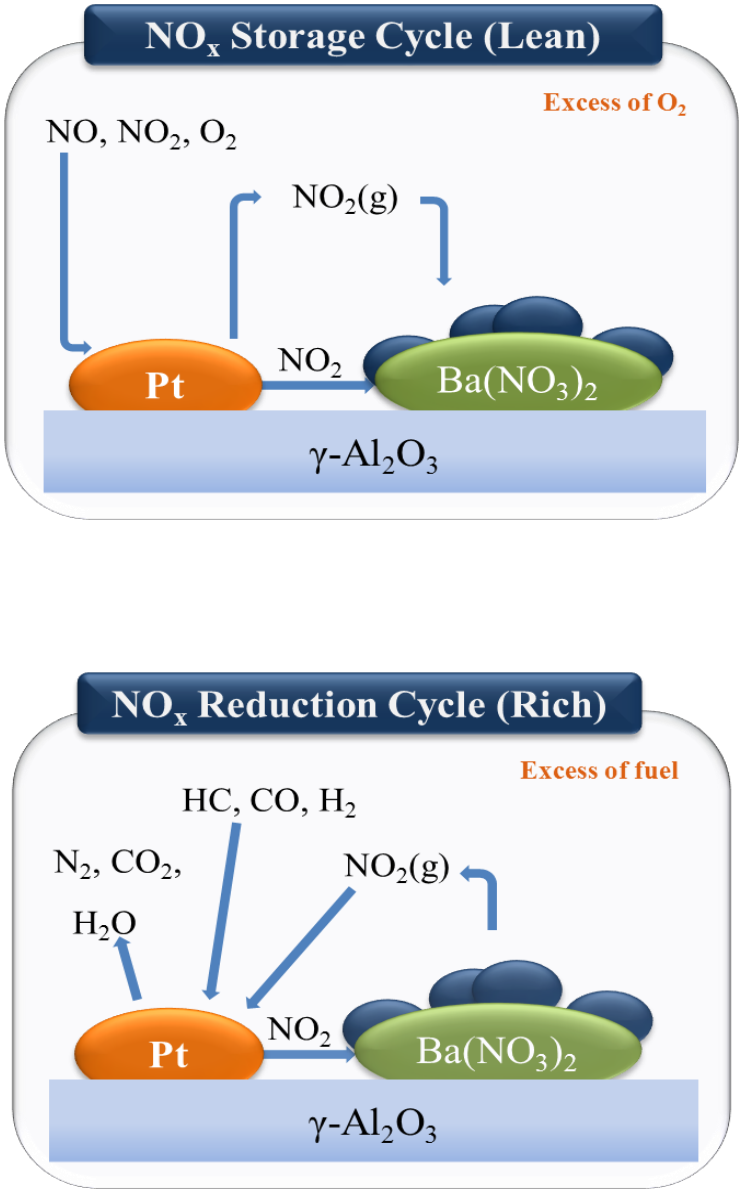

Figure 4. Scheme for NSR reaction mechanism [27].

Chapter 3. Experimental

3.1. Preparation of catalyst

3.1.1. Synthesis of Hydrotalcite

Hydrotalcite with different Mg/Al molar ratio was prepared by using co-precipitation method [36-39]. To synthesize hydrotalcite, two different types of solutions were needed. Solution A consisted of $Mg(NO_3)_2 \cdot 6H_2O$ precursor and $Al(NO_3)_3 \cdot 9H_2O$ precursor in 200 mL distilled water, and Solution B consisted of Na_2CO_3 and NaOH in 200 mL distilled water. After mixing each solution, solution B was added to solution A by keeping drop-wise rate, temperature at 80 ℃, and pH value as 10 ± 0.5. The mixture cooled down with continuous stirring until the temperature reached room temperature. Then, the product was filtered with distilled water until pH=7, followed by drying at 110 ℃ in an oven overnight. The dried sample was ground and calcined at 800 ℃ for 6 hours in a muffle furnace.

3.1.2. Preparation of Pt-BaO/Support catalysts

A 20wt% Ba was loaded on each support which is Al_2O_3, MgAl (1:9), MgAl (2:8), MgAl (3:7), MgAl (4:6), and MgAl (5:5) by using incipient wetness impregnation method with $Ba(NO_3)_2$. Then, a 2 wt% Pt was also loaded on the samples with $Pt(NH_3)_4(NO_3)_2$ using the same method. After impregnation, all samples were calcined at 500 ℃, 650 ℃, and 800 ℃ in 15 vol % O_2/N_2 for 2 hours each.

3.2. Characterization of the prepared catalysts

3.2.1. N_2 adsorption-desorption

The specific surface areas of the catalysts were analyzed using N_2 adsorption-desorption apparatus (Micrometritics ASAP 2010) at constant temperature (77K). All samples were pretreated at 250 ℃ for at least 4 hours in evacuation condition, and the specific surface areas of the samples were measured using BET method.

3.2.2. X-ray diffraction (XRD)

For the analysis of bulk properties of the catalysts, the powder X-ray diffraction experiment was carried out on a high power X-ray diffractometer (Rigaku Corp.) using Cu Kα as a radiation source at 40 kV and 400 mA. The scan rate was fixed as 2.3 degree/min in the range of 10-80 degree.

3.2.3. Inductively coupled plasma (ICP-AES)

To confirm loaded amount of Pt and Ba and the ratio of Mg and Al,

ICP-AES was tested (PerkinElmer/Optima-4300 DV). The weight of the each sample was about 0.03 g, and the sample dissolved in 5 mL aqua regia. The solution was diluted with distilled water. Then, ICP-AES analysis was performed with the solution.

3.2.4. Temperature-programmed desorption (TPD)

Thermal stability of stored NOx on each catalyst was examined by NO_2-TPD in a quartz fixed bed reactor with NOx analyzer (Thermo electron Corp., 42i-HL). Each sample was pretreated and dosed with 5000 ppm NO_2. After the dosing step, the catalyst was cooled down at room temperature, then, desorbed up to 700 ℃.

3.2.5. FT-IR and Chemisorption

FT-IR experiment was carried out (MIDAC Corp.) to get information of interaction between Pt and support. Pellet was made with about 0.07 g of sample and pretreated with H_2 for reduction of sample. After all pretreatment steps, CO gas was dosed on the pellet then FT-IR spectra were taken under the vacuum. Also, CO chemisorption was tested to get information on

dispersion of Pt on the support. CO gas was adsorbed on the pretreated sample at 35 ℃, and dispersion data was obtained on each pressure.

3.2.6. Transmission electron microscopy (TEM)

In order to analyze structure and dispersion of the samples, transmission electron microscope (TEM, JEM-2100 F) was used. The sample solution which was dissolved with small amount of catalysts in ethanol was dropped on a carbon-coated Cu grid and dried at room temperature. Also, Energy dispersive spectroscopy (EDS, Oxford) was also measured to confirm atoms in the TEM image.

3.3. Activity test – NOx Storage Reduction (NSR)

NOx storage reduction reaction was performed in a fixed-bed reactor under continuous lean-rich cycles. Total 4 cycles of 1 min rich and 4 min lean were applied, and about 0.05 g of sample was used to conduct the reaction. NOx concentrations in both inlet and outlet were measured with a NOx analyzer (Thermo electron Corp., 42i-HL). NOx uptake was defined as total adsorbed NOx amount when outlet NOx concentration was 60 ppm that is 20%

of the inlet NOx concentration. Then, it was normalized by the weight of the sample. The mixture gas consisted of a continuous flow of 10 % CO_2 with N_2 balance and either 4 % H_2 (rich condition) or 300 ppm of NO and 10 % O_2 (lean condition). The total flow was 200 mL/min, and each gas was controlled by mass flow controllers (MKS). The reaction temperature was from 500 ℃ to 250 ℃ in decrements of 50 ℃ per each step.

Chapter 4. Results and discussion

4.1. Fresh samples

Synthesized hydrotalcites with different Mg/Al molar ratios were calcined at 800 ℃ for 6 hours in a muffle furnace and then used as NSR catalyst support. 20wt% Ba and 2 wt% Pt were loaded on the supports, and each catalyst was calcined at 500 ℃ for 2 hours in 15% O_2/N_2. These samples were called fresh samples, and to confirm the value of loaded active components and check the Mg/Al ratios, we conducted ICP experiment. The results are presented in Table 2. Overall, the values of the samples are mostly consistent with calculated values.

Specific surface area results are indicated in Table 3. By increasing the amount of Mg, specific surface area also increases until MgAl molar ratio is 4:6; these results are in agreement with previous study [11]. However, when the MgAl ratio is 5:5, specific surface area decreases. After active components were loaded on the samples, specific surface area slightly decreases comparing with the supports and shows the same trend with supports. Figure 5 shows XRD patterns of the supports. As Mg contents increase, the patterns of MgO phases increase. Figure 6 gives the

information that HT-supported catalysts show the same XRD patterns with the supports, and Al_2O_3-supported sample shows undecomposed $Ba(NO_3)_2$ phases. We did not show MgAl (1:9)-supported sample because the catalyst show inferior activity on NOx storage reduction reaction which will be explained later.

Table 2. Inductively Coupled Plasma (ICP) results of the samples

	Mg/Al	BaO/(Support+BaO) (%)	Pt/(Pt+BaO+support) (%)
MgAl (1:9)	**0.13** (0.11)	24.16	2.70
MgAl (2:8)	**0.26** (0.25)	19.21	2.35
MgAl (3:7)	**0.48** (0.43)	18.31	2.50
MgAl (4:6)	**0.73** (0.67)	17.78	2.70
MgAl (5:5)	**1.16** (1.00)	17.80	2.78
γ-Al_2O_3	-	24.29	2.33

Table 3. Specific surface area of the catalysts

Unit : m^2/g

Catalysts	S_{BET}
γ-Al_2O_3	321[(a)]
MgAl (1:9)	89[(b)]
MgAl (2:8)	106[(b)]
MgAl (3:7)	126[(b)]
MgAl (4:6)	145[(b)]
MgAl (5:5)	118[(b)]
2wt% Pt-20wt% BaO/γ-Al_2O_3	192[(c)]
2wt% Pt-20wt% BaO/MgAl (1:9)	30[(c)]
2wt% Pt-20wt% BaO/MgAl (2:8)	60[(c)]
2wt% Pt-20wt% BaO/MgAl (3:7)	92[(c)]
2wt% Pt-20wt% BaO/MgAl (4:6)	98[(c)]
2wt% Pt-20wt% BaO/MgAl (5:5)	106[(c)]

(a) Calcination at 550 ^oC, 2 hrs in air, (b) Calcination at 800 ^oC, 6 hrs in air,

(c) Calcination at 550 ^oC, 2 hrs in 15% O_2/N_2

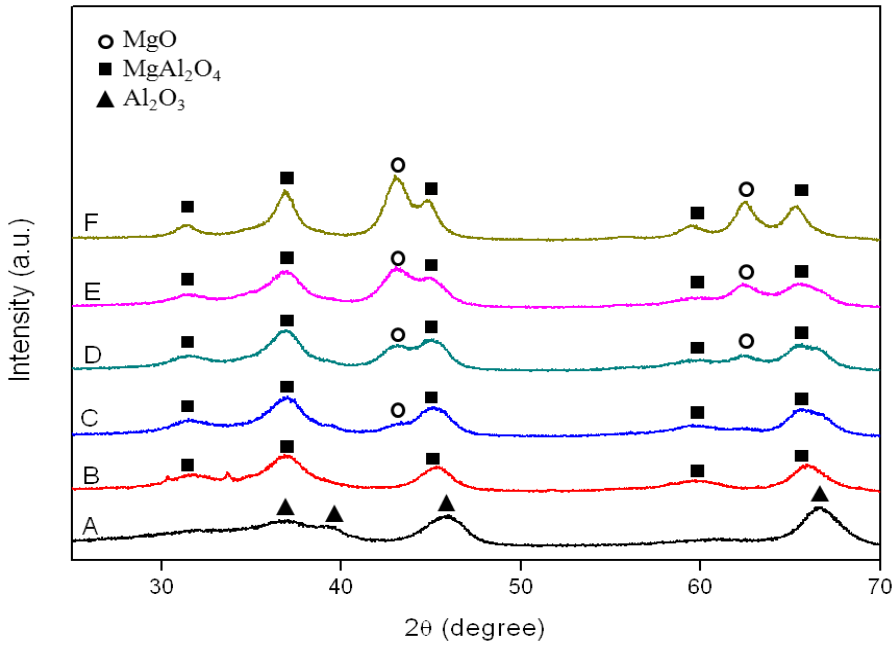

Figure 5. XRD patterns of the supports (A: Al_2O_3, B: MgAl (1:9), C: MgAl (2:8), D: MgAl (3:7), E: MgAl (4:6), F: MgAl (5:5), calcination at 800 ℃ for 6 hrs).

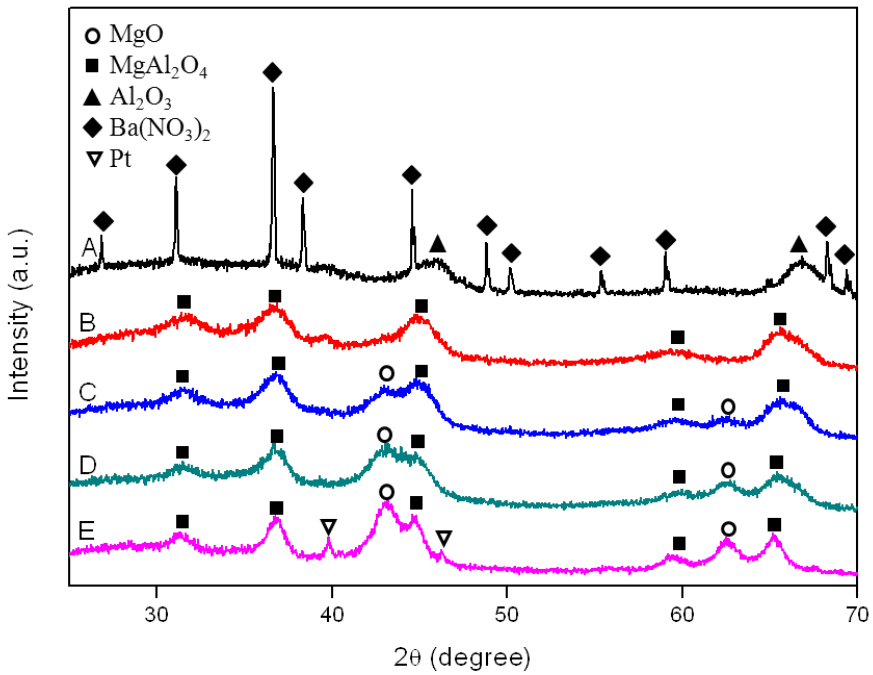

Figure 6. XRD patterns of the fresh samples (A: 2wt% Pt-20wt% BaO/ Al_2O_3, B: 2wt% Pt-20wt% BaO/MgAl (2:8), C: 2wt% Pt-20wt% BaO/ MgAl (3:7), D: 2wt% Pt-20wt% BaO/MgAl (4:6), E: 2wt% Pt-20wt% BaO/MgAl (5:5)).

Figure 7 suggests that HT-supported catalysts show much more excellent NOx storage performance than Al_2O_3-supported one. Due to poor NSR reaction activities of both MgAl (1:9)-supported catalyst, we exclude further analysis on MgAl (1:9)-supported catalyst. We get to the point; the reaction result can be explained by (i) Ba effect and (ii) Pt dispersion. The former reason can be explained by Figure 8. As indicated in Figure 8, thermal stability of nitrate species formed on 20wt% BaO/HT samples is superior to that of Al_2O_3. Especially, 20wt% BaO/MgAl (2:8) sample shows the best thermal stability. This result is in agreement with NSR reaction result which shows outstanding NOx storage performance of 2wt% Pt-20wt% BaO/MgAl (2:8) catalyst. The further reason would be supported by Figure 9, 10, 11 and Table 4. Figure 9 shows STEM images. Through these images, we can see well dispersed Pt on the supports; we confirmed that white spots are Pt particles using EDS. Especially, we checked that the particle size of Pt on HTs is smaller than that of Al_2O_3 through TEM data indicated in Figure 10; that is, Pt particle size in Al_2O_3-supported catalyst is about 3.39 nm, but one in HT-supported catalyst is about 1.99 nm. Due to this reason, HT-supported catalysts show better NOx storage performance than Al_2O_3-supported one. Another evidence for proving existence of well dispersed Pt is in Figure 11. With FT-IR experiment, we could get the information between Pt and

support; this technique is well known for a long time. FT-IR data shows that the amount of adsorbed CO on Pt particles increases by increasing the amount of Mg; The peaks at 2053 and 1669-1870 cm^{-1} refer to linear CO and bridged CO, respectively [40-42]. That means the existence of well dispersed Pt due to increment of Mg contents. FT-IR result of MgAl (5:5)-supported catalyst was excluded in this paper. Table 4 describes also the same word with FT-IR data other than MgAl (5:5)-supported catalyst. Dispersion of its sample decreases compared to other hydrotalcite supports. This is related to the reaction result showing inferior activity on MgAl (5:5)-supported catalyst.

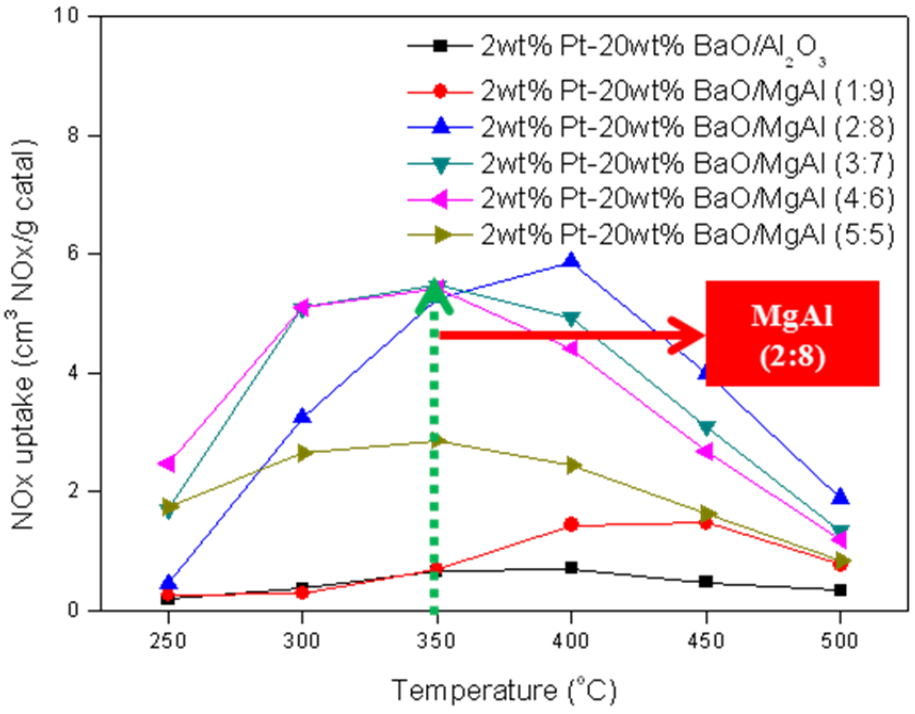

Figure 7. NOx storage performance of the fresh samples.

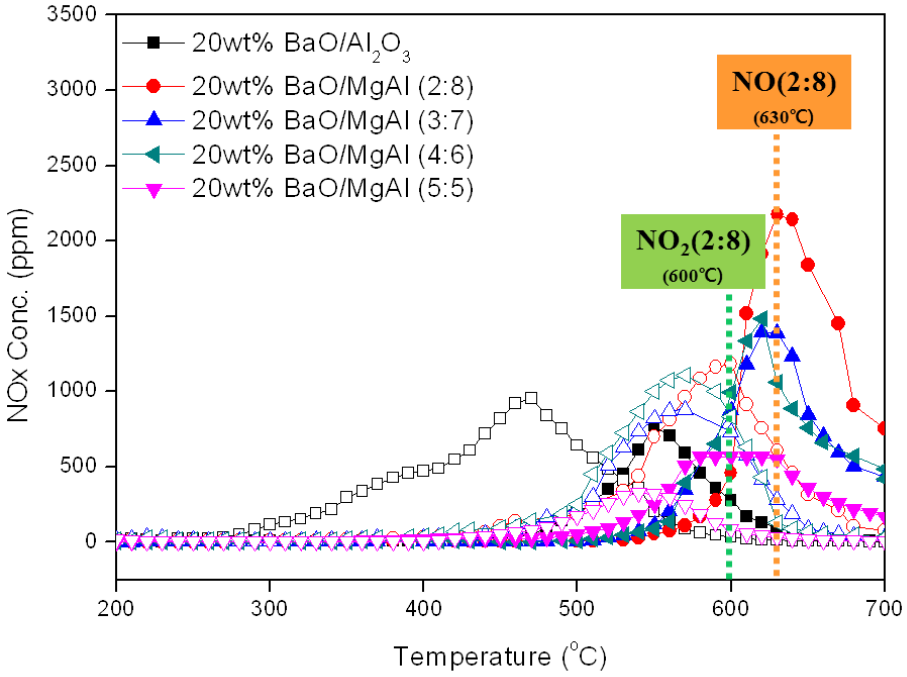

Figure 8. NO_2-TPD results of 20wt% BaO/Supports (Open symbol : NO_2, Closed symbol : NO).

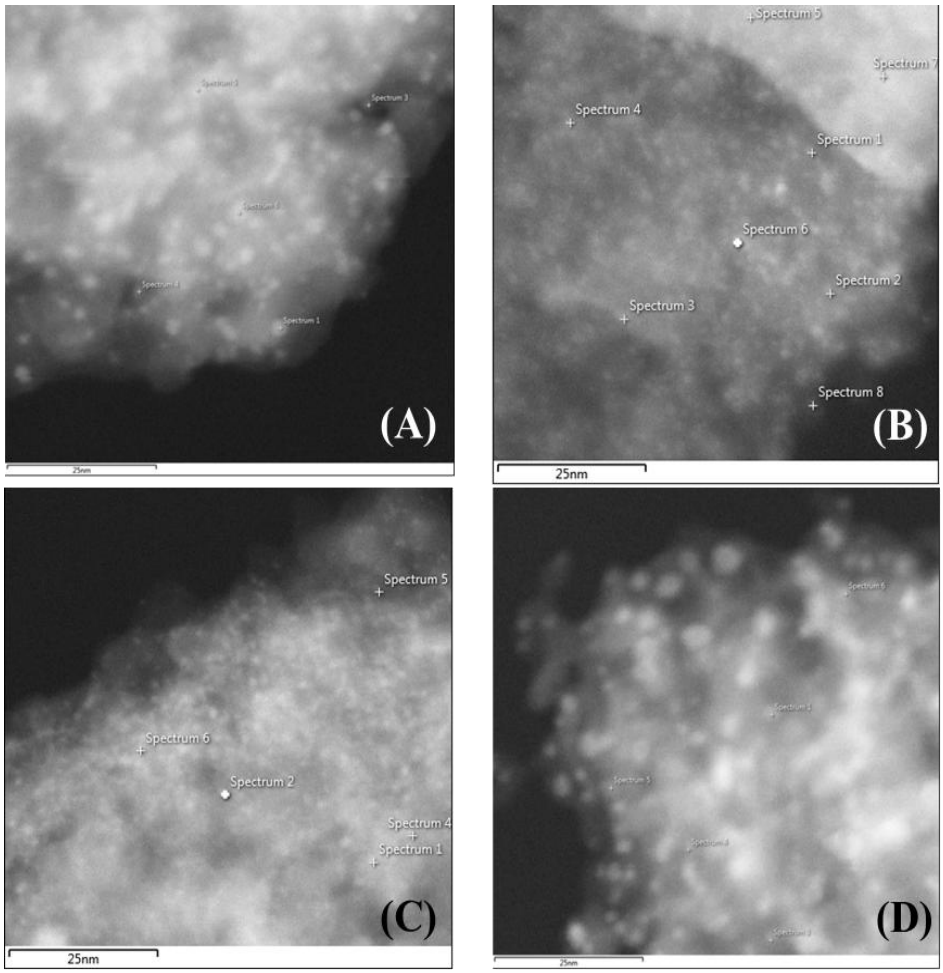

Figure 9. STEM images of (A) 2wt% Pt-20wt% BaO/Al_2O_3, (B) 2wt% Pt-20wt% BaO/MgAl (2:8), (C) 2wt% Pt-20wt% BaO/MgAl (3:7), and (D) 2wt% Pt-20wt% BaO/MgAl (4:6), (All samples were calcined at 500 ℃ for 2 hrs in 15% O_2/N_2).

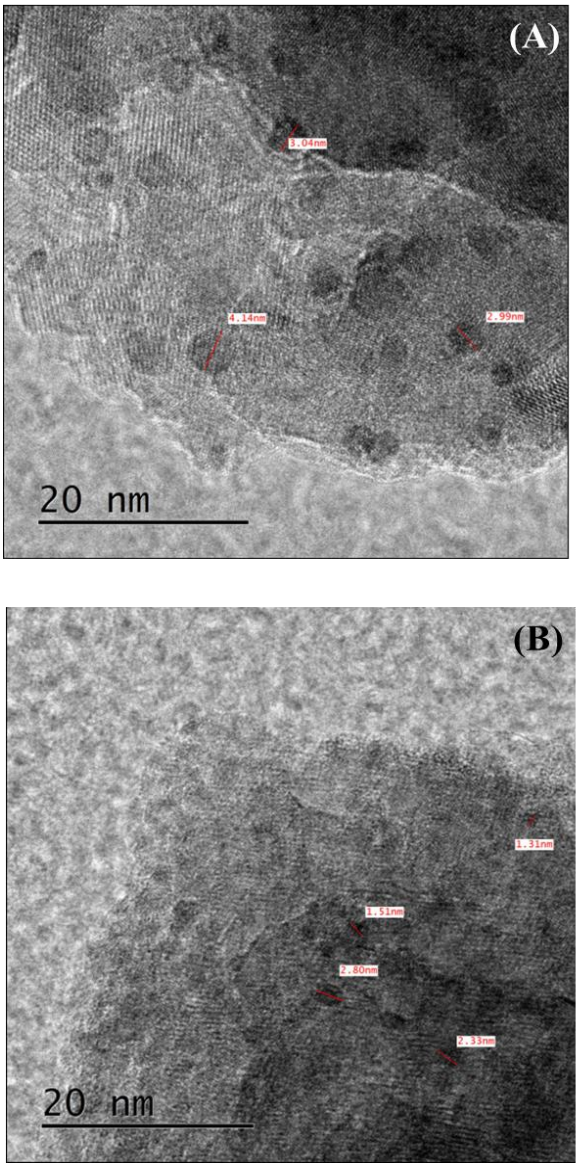

Figure 10. TEM images of (A) 2wt% Pt-20wt% BaO/Al_2O_3 and (B) 2wt% Pt-20wt% BaO/MgAl (4:6), (All samples were calcined at 500 ℃ for 2 hrs in 15% O_2/N_2).

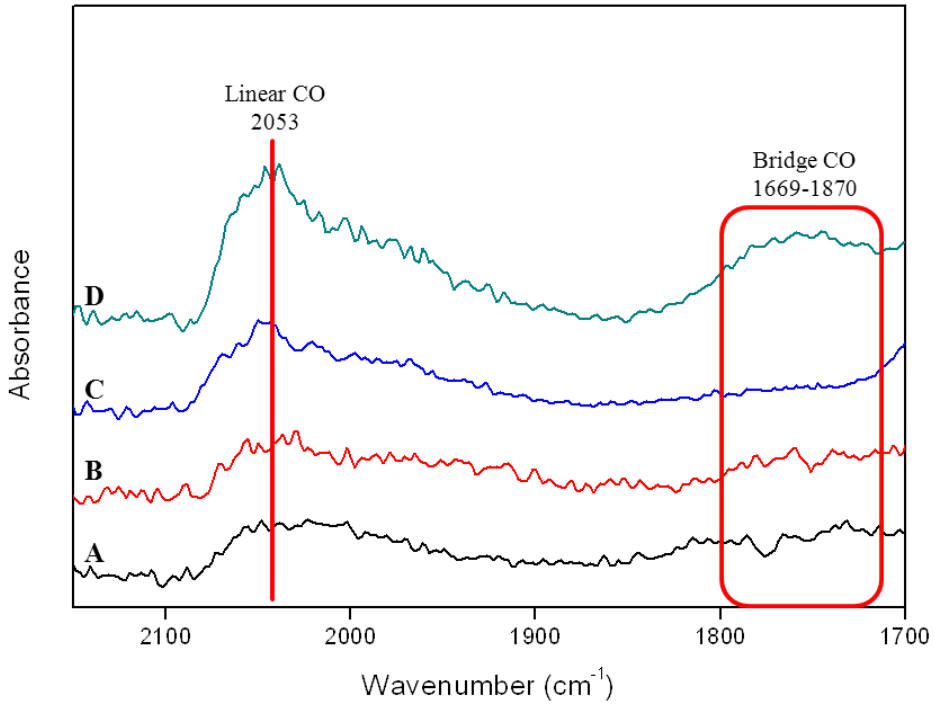

Figure 11. FT-IR spectra of the fresh samples (A: 2wt%Pt-20wt% BaO/Al_2O_3, B: 2wt%Pt-20wt%BaO/MgAl (2:8), C: 2wt%Pt-20wt% BaO/MgAl (3:7), D: 2wt%Pt-20wt%BaO/MgAl (4:6), Adsorbed gas : CO).

Table 4. Dispersion data of the fresh samples (Adsorbed gas : CO)

Catalysts	**Dispersion (%)**
2wt% Pt-20wt% BaO/γ-Al_2O_3	18
2wt% Pt-20wt% BaO /MgAl (2:8)	20
2wt% Pt-20wt% BaO /MgAl (3:7)	24
2wt% Pt-20wt% BaO /MgAl (4:6)	46
2wt% Pt-20wt% BaO/MgAl (5:5)	13

4.2. Aged samples

There are two types of aged samples. One was aged at 650 ℃, and the other was aged at 800 ℃ for 2 hour under 15% O_2/N_2 flow, respectively. Specific surface area of two aged samples decreases compared with fresh samples as indicated in Table 5. Also, as aged temperature is getting higher, specific surface area decreases.

Figure 12 shows NSR reaction results of the samples aged at 650 ℃. It shows that the activities of Al_2O_3-supported catalyst, MgAl (2:8)-supported catalyst and MgAl (5:5)-supported catalyst are deteriorated. However, the activities of MgAl (3:7)-supported catalyst and MgAl (4:6)-supported catalyst are superior even though their activities are poor at low temperature. This fact can be explained by XRD data in Figure 13. All XRD patterns are almost same with previous XRD data in Figure 5 except that XRD patterns of Pt occur. Especially, Al_2O_3-supported catalyst shows the worst activity due to a lot of sintered Pt. Similar tendency is shown in the samples aged at 800 ℃. As shown in Figure 14, Al_2O_3-supported catalyst, MgAl (2:8)-supported catalyst, and MgAl (5:5)-supported catalyst still show deteriorated activity on NOx storage. Deactivation extent of Al_2O_3-supported sample is especially large among the samples. The reasons are (i) formation of $BaAl_2O_4$ (ii) sintering of

Pt. As indicated in Figure 15, thermal aging at high temperature results in formation of $BaAl_2O_4$ phases only in Al_2O_3. However, there are no $BaAl_2O_4$ phases in HT-supported samples. The sample especially, MgAl (4:6)-supported one shows superior NOx storage performance at high temperature. Through Figure 15 and Table 6 we can get information about sintered Pt and the reason why NOx storage performance of MgAl (2:8)-supported catalyst is deactivated. In Figure 15, the XRD patterns of all samples are presented, and we calculated the area of Pt on each sample and describe in Table 6. The area of Pt in Al_2O_3-supported sample is larger than other samples, and the particle size of Pt is 30.4 nm; this paper only shows the area. The area of Pt in HT-supported catalysts is smaller than Al_2O_3-supported one, and by increasing Mg/Al ratio, the area decreases. As a result of measurement of Pt particle size in HT-supported catalysts, the sizes are larger than Al_2O_3-supported one although the area of Pt in HT-supported catalysts is much smaller than Al_2O_3-supported one. This means that partially sintered particles of Pt are detected by XRD, and other Pt particles exist with small particle size, so they are not detected by XRD. In other words, dispersed Pt on HT supports is not sintered a lot even at high temperature.

When we see Figure 12 and Figure 14, we can find that there is one difference between 650 ℃ samples and 800 ℃ samples. The temperature

where the activity is maximum is shifted to higher temperature from 400 ℃ to 450 ℃. By G. Fornasari et al., increment of Mg contents leads thermal stability [17]. This comment is consistent with our data.

Table 5. Specific surface area of aged samples

Unit : m^2/g

Catalysts	S_{BET}
2wt% Pt-20wt% BaO/γ-Al_2O_3	141[(a)] 120[(b)]
2wt% Pt-20wt% BaO/MgAl(2:8)	49[(a)] 51[(b)]
2wt% Pt-20wt% BaO/MgAl(3:7)	68[(a)] 61[(b)]
2wt% Pt-20wt% BaO/MgAl(4:6)	81[(a)] 65[(b)]
2wt% Pt-20wt% BaO/MgAl(5:5)	96[(a)] 54[(b)]

(a) Calcination at 650 ^oC, 2 hrs in 15% O_2/N_2, (b) Calcination at 800 ^oC, 2 hrs in 15% O_2/N_2

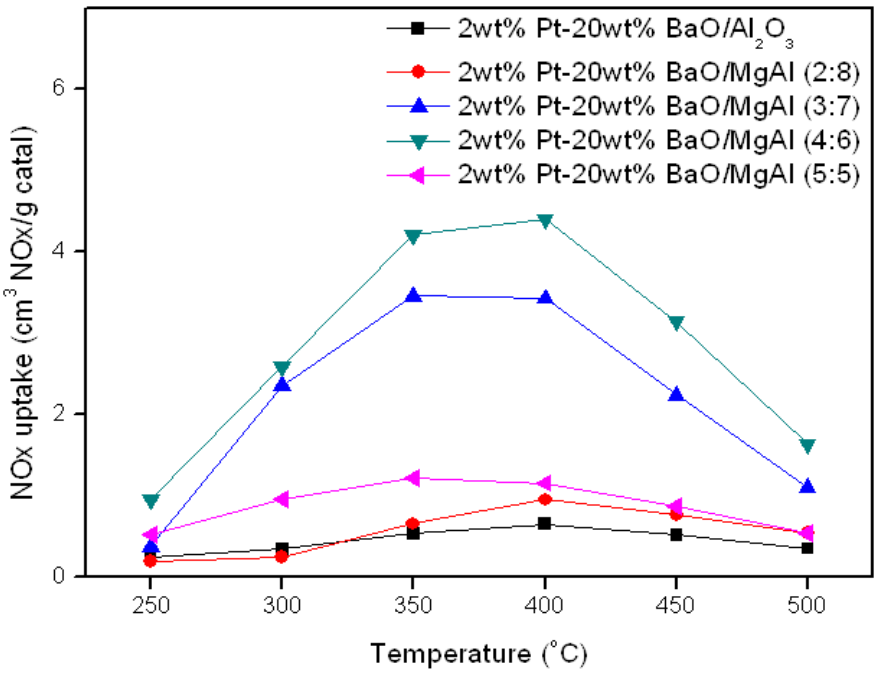

Figure 12. NOx storage performance of the aged samples (Aging temperature : 650 ℃).

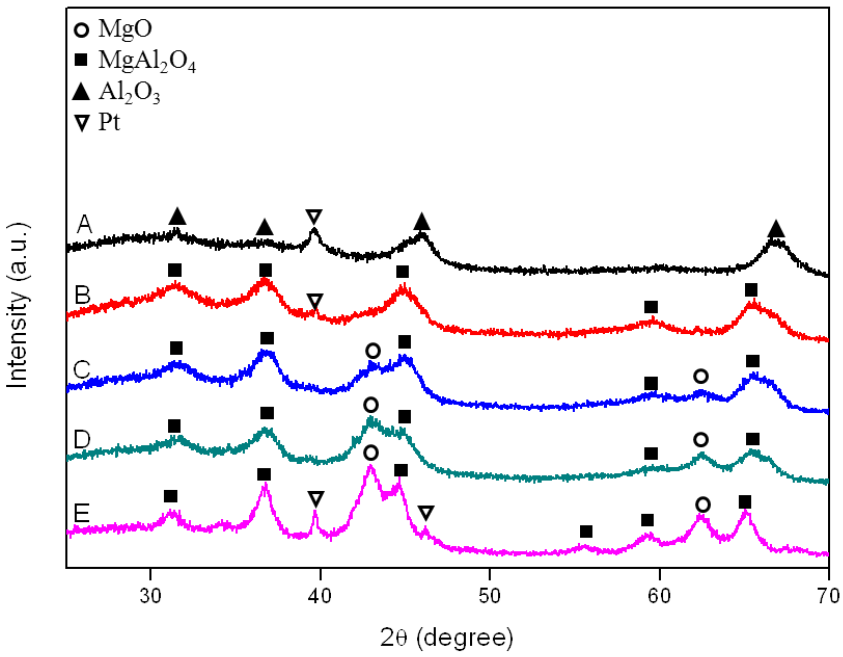

Figure 13. XRD patterns of the aged samples (calcination at 650 ℃, A: 2wt% Pt-20wt% BaO/Al_2O_3, B: 2wt% Pt-20wt% BaO/MgAl (2:8), C: 2wt% Pt-20wt% BaO/MgAl (3:7), D: 2wt% Pt-20wt% BaO/MgAl (4:6), E: 2wt% Pt-20wt% BaO/MgAl (5:5)).

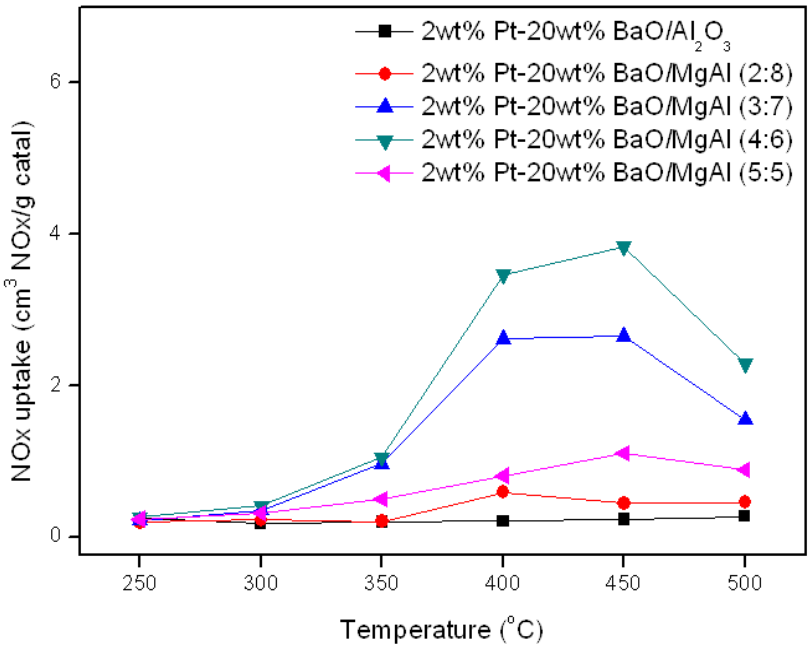

Figure 14. NOx storage performance of the aged samples (Aging temperature : 800 ℃).

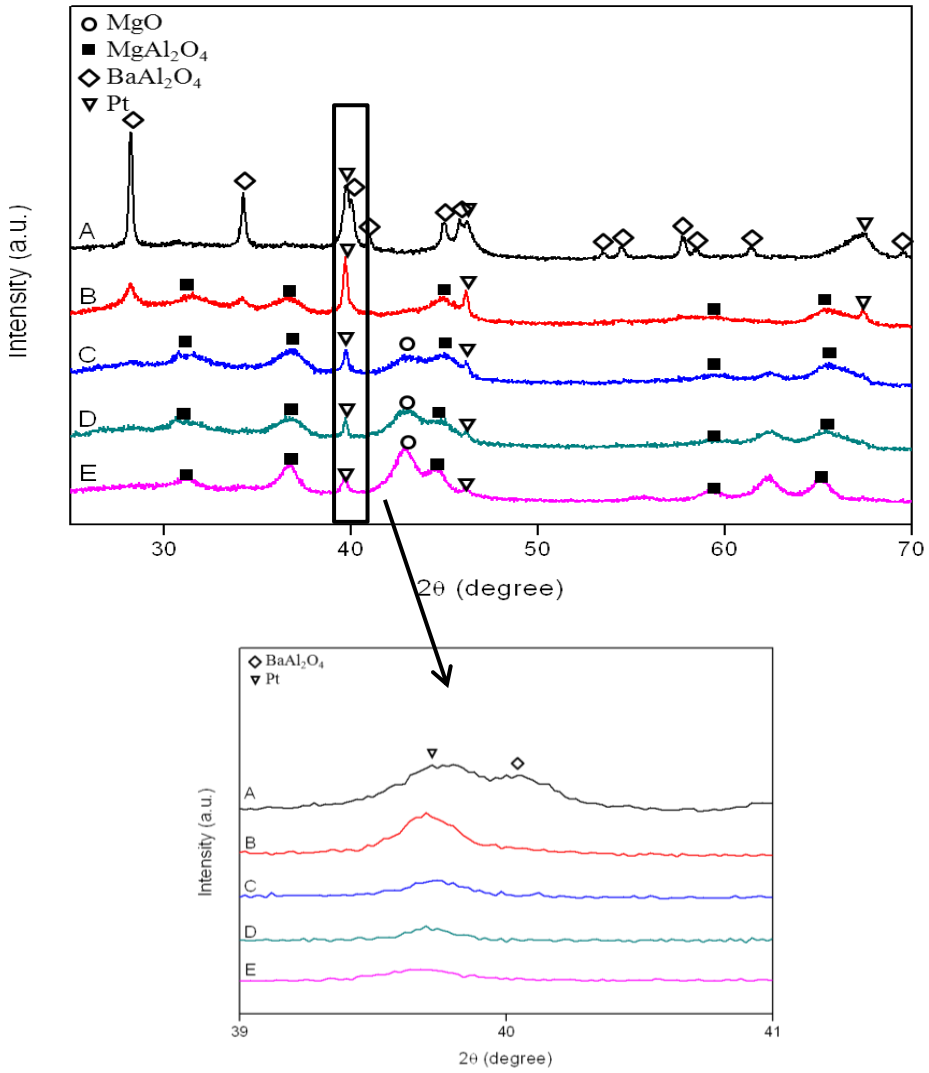

Figure 15. XRD patterns of the aged samples (calcination at 800 ℃, A: 2wt% Pt-20wt% BaO/Al_2O_3, B: 2wt% Pt-20wt% BaO/MgAl (2:8), C: 2wt% Pt-20wt% BaO/MgAl (3:7), D: 2wt% Pt-20wt% BaO/MgAl (4:6), E: 2wt% Pt-20wt% BaO/MgAl (5:5)).

Table 6. XRD peak area of Pt

Catalysts	Area
2wt% Pt-20wt% BaO/Al_2O_3	16184
2wt% Pt-20wt% BaO/MgAl (2:8)	8118
2wt% Pt-20wt% BaO/MgAl (3:7)	3085
2wt% Pt-20wt% BaO/MgAl (4:6)	1925
2wt% Pt-20wt% BaO/MgAl (5:5)	1283

4.3. Pt/HT samples

To check whether hydrotalcite has NOx storage performance by itself, we examined NO_2-TPD using only hydrotalcites. Also, we prepared Pt/HT catalysts without Ba loading to conduct NSR reaction test. As shown in Figure 16, we check that hydrotalcite can store NOx without storage elements at low temperature. Among all samples, MgAl (2:8) sample shows the best NOx storage ability, and other ratio samples still show lots of NOx storage performance compared with Al_2O_3. Through this result, we confirm that hydrotalcite has the ability of NOx storage at low temperature. Previous study mentioned that by increasing Mg/Al atomic ratio, NOx storage performance increased [17]. Our experiment data indicated in Figure 17 says the same word that MgAl (4:6) sample shows the best activity followed by MgAl (3:7) and MgAl (2:8). With NO_2-TPD experiment and NSR reaction test, we can be sure that hydrotalcite can store NOx at low temperature without storage elements such as Ba.

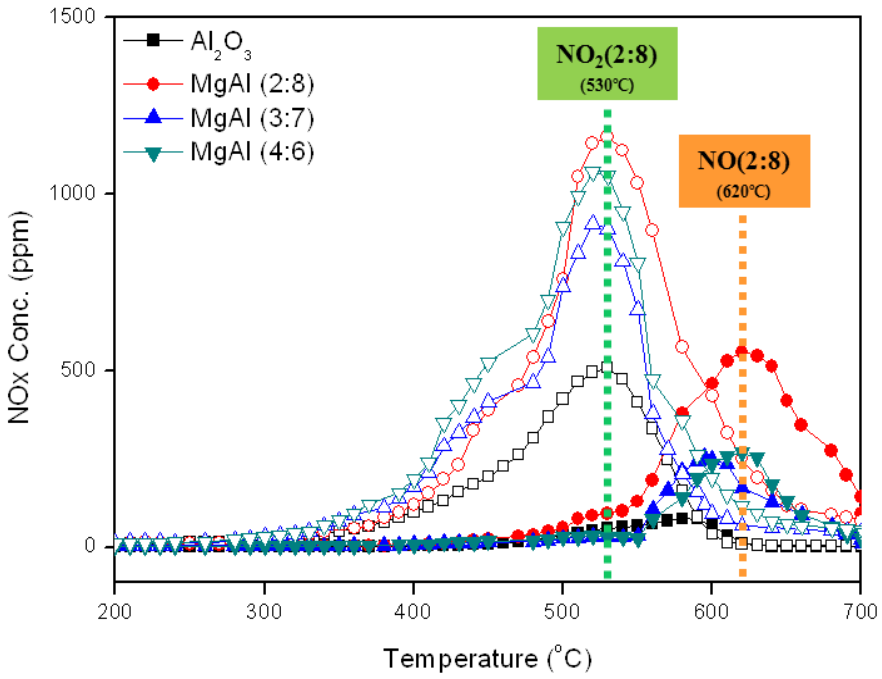

Figure 16. NO_2-TPD results of the supports (Open symbol : NO_2, Closed symbol : NO).

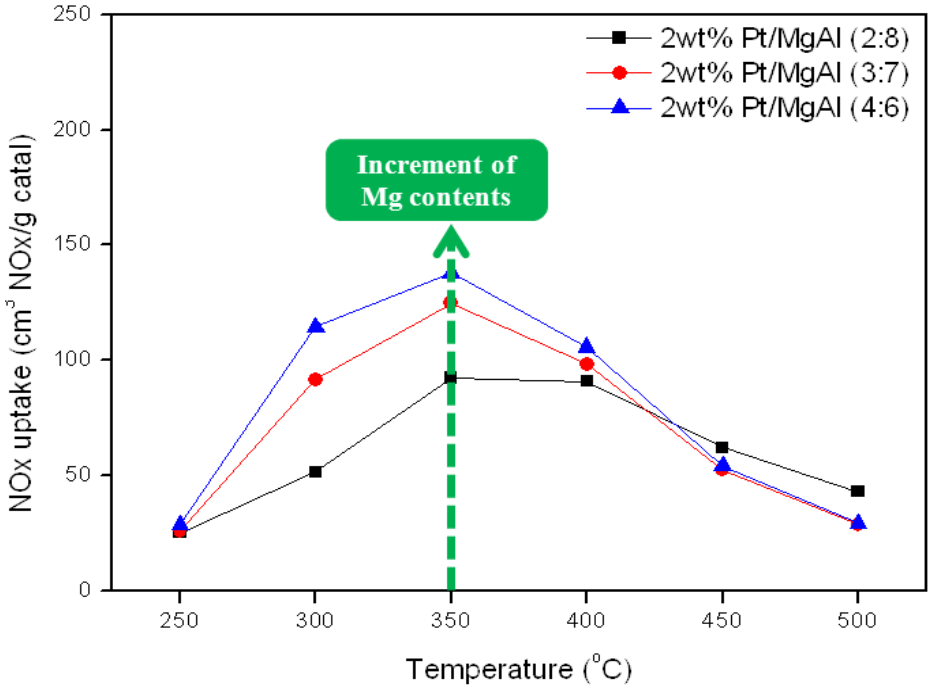

Figure 17. NOx storage performance of Pt/HT catalysts (calcination at 500 ℃).

Chapter 5. Conclusions

In this work, various characteristics of HT-supported catalysts were analyzed compared to Al_2O_3-supported catalysts. The prepared catalysts were calcined at 500 ℃ (Fresh), 650 ℃, and 800 ℃ (Aged) for 2 hours.

At fresh samples, the activities of HT-supported catalysts were superior to Al_2O_3-supported one, especially MgAl (2:8)-supported catalyst, and the active temperature range of HT-supported catalysts was wide compared to Al_2O_3-supported catalyst; the active temperature region of Al_2O_3-supported catalyst is about 300 ℃ ~ 350 ℃. Similar results showed in the aged samples calcined at both 650 ℃ and 800 ℃. Two types of aged samples showed improved NOx storage performance at high temperature even though their NOx storage performance was poor at low temperature. Also, by calcining at high temperature (650 ℃ and 800 ℃), the temperature where the activity is maximized was shifted to high temperature from 400 ℃ to 450 ℃. These mean HT-supported catalysts are thermally stable. In conclusion, using hydrotalcite as support leads to inhibition of sintering of Pt and improvement of dispersion of Pt. In other words, thermal stability is improved. That is why the NOx storage performance of HT-supported catalysts is superior to Al_2O_3-supported one. Among the various MgAl molar

ratios, 4:6 is the optimum ratio to be used. Also, hydrotalcite has the ability for storing NOx without storage elements at low temperature. We confirmed the fact through the experiment. Because of all reasons mentioned, HT-supported catalysts showed the best performance for the NOx storage, especially MgAl (4:6).

References

[1] J.C. Clerc, Applied Catalysis B: Environmental, 10 (1996) 99.

[2] S.R. Katare, J.E. Patterson and P.M. Laing, Ind. Eng. Chem. Res., 46 (2007) 2445.

[3] P. Zelenka, W. Cartellieri and P. Herzog, Applied Catalysis B-Environmental, 10 (1996) 3.

[4] X. Auvray, T. Pingel, E. Olsson and L. Olsson, Applied Catalysis B-Environmental, 129 (2013) 517.

[5] S. Roy and A. Baiker, Chemical Reviews, 109 (2009) 4054.

[6] M.V. Twigg, Applied Catalysis B-Environmental, 70 (2007) 2.

[7] A. Scotti, I. Nova, E. Tronconi, L. Castoldi, L. Lietti and P. Forzatti, Ind. Eng. Chem. Res., 43 (2004) 4522.

[8] V. Vestreng, L. Ntziachristos, A. Semb, S. Reis, I.S.A. Isaksen and L. Tarrason, Atmospheric Chemistry and Physics, 9 (2009) 1503.

[9] N.D. Hutson, S.A. Speakman and E.A. Payzant, Chemistry of Materials, 16 (2004) 4135.

[10] A. Vaccari, Catalysis Today, 41 (1998) 53.

[11] R. Salomao, L.M. Milena, M.H. Wakamatsu and V.C. Pandolfelli, Ceramics International, 37 (2011) 3063.

[12] T. Lopez, P. Bosch, E. Ramos, R. Gomez, O. Novaro, D. Acosta and F. Figueras, Langmuir, 12 (1996) 189.

[13] W.T. Reichle, S.Y. Kang and D.S. Everhardt, Journal of Catalysis, 101 (1986) 352.

[14] F. Cavani, F. Trifirò and A. Vaccari, Catalysis Today, 11 (1991) 173.

[15] S.J. Park, H.A. Ahn, I.J. Heo, I.S. Nam, J.H. Lee, Y.K. Youn and H.J. Kim, Topics in Catalysis, 53 (2010) 57.

[16] S. Roy, N. van Vegten and A. Baiker, Journal of Catalysis, 271 (2010) 125.
[17] G. Fornasari, R. Glockler, M. Livi and A. Vaccari, Applied Clay Science, 29 (2005) 258.
[18] D.H. Kim, K. Mudiyanselage, J. Szanyi, H. Zhu, J.H. Kwak and C.H.F. Peden, Catalysis Today, 184 (2012) 2.
[19] F. Prinetto, M. Manzoli, S. Morandi, F. Frola, G. Ghiotti, L. Castoldi, L. Lietti and P. Forzatti, Journal of Physical Chemistry C, 114 (2010) 1127.
[20] G. Fornasari, F. Trifirò, A. Vaccari, F. Prinetto, G. Ghiotti and G. Centi, Catalysis Today, 75 (2002) 421.
[21] B.M. Shakya, M.P. Harold and V. Balakotaiah, Catalysis Today, 184 (2012) 27.
[22] N. Takahashi, S. Matsunaga, T. Tanaka, H. Sobukawa and H. Shinjoh, Applied Catalysis B-Environmental, 77 (2007) 73.
[23] A. Russell and W.S. Epling, Catal. Rev.-Sci. Eng., 53 (2011) 337.
[24] J. Kim, C. Kim and S.J. Choung, Catalysis Today, 185 (2012) 296.
[25] L. Lizarraga, S. Souentie, A. Boreave, C. George, B. D'Anna and P. Vernoux, Environmental Science & Technology, 45 (2011) 10591.
[26] R.J. Farrauto and K.E. Voss, Applied Catalysis B-Environmental, 10 (1996) 29.
[27] I.J. Jang, (2012).
[28] P.G. Savva and C.N. Costa, Catal. Rev.-Sci. Eng., 53 (2011) 91.
[29] J. Due-Hansen, S.B. Rasmussen, E. Mikolajska, M.A. Bañares, P. Ávila and R. Fehrmann, Applied Catalysis B: Environmental, 107 (2011) 340.

[30] G. Busca, L. Lietti, G. Ramis and F. Berti, Applied Catalysis B: Environmental, 18 (1998) 1.
[31] T. Szailer, J.H. Kwak, D.H. Kim, J. Szanyi, C.M. Wang and C.H.F. Peden, Catalysis Today, 114 (2006) 86.
[32] N.N. Hou, Y.X. Zhang and M. Meng, Journal of Physical Chemistry C, 117 (2013) 4089.
[33] S. Roy, N. van Vegten, N. Maeda and A. Baiker, Applied Catalysis B-Environmental, 119 (2012) 279.
[34] N.A. Ottinger, T.J. Toops, N. Ke, B.G. Bunting and J. Howe, Applied Catalysis B-Environmental, 101 (2011) 486.
[35] A.E. Palomares, A. Uzcategui and A. Corma, Catalysis Today, 137 (2008) 261.
[36] Q. Wang, H.H. Tay, Z.H. Guo, L.W. Chen, Y. Liu, J. Chang, Z.Y. Zhong, J.Z. Luo and A. Borgna, Applied Clay Science, 55 (2012) 18.
[37] J.Y. Shen, J.M. Kobe, Y. Chen and J.A. Dumesic, Langmuir, 10 (1994) 3902.
[38] A. Wajler, H. Tomaszewski, E. Drozdz-Ciesla, H. Weglarz and Z. Kaszkur, Journal of the European Ceramic Society, 28 (2008) 2495.
[39] P. Sangeetha, P. Seetharamulu, K. Shanthi, S. Narayanan and K.S.R. Rao, Journal of Molecular Catalysis a-Chemical, 273 (2007) 244.
[40] A. Tomita, K. Shimizu, K. Kato, T. Akita and Y. Tai, Journal of Physical Chemistry C, 117 (2013) 1268.
[41] G. Busca, E. Finocchio and V.S. Escribano, Applied Catalysis B-Environmental, 113 (2012) 172.
[42] A. Virnovskaia, S. Morandi, E. Rytter, G. Ghiotti and U. Olsbye, Journal of Physical Chemistry C, 111 (2007) 14732.

초 록

일반적으로 디젤 엔진은 가솔린 엔진에 비해 과잉 산화조건에서 연소가 진행된다. 따라서 기존의 삼원촉매로는 대기 중에 배출되는 질소 산화물을 효과적으로 환원하여 제거하는 데에 어려움이 있다. 질소 산화물을 효율적으로 제거하기 위한 방법 중 질소 산화물 흡장 환원 기술이 대표적이며 주로 사용되는 촉매는 Pt-BaO/Al_2O_3 이다. 그러나 이 촉매는 활성이 우수하지만 열적 내구성이 우수하지 못하며 활성온도 범위가 좁은 단점이 있다. 본 연구에서는 이를 개선하기 위한 방법으로 Mg과 Al의 혼합 산화물인 하이드로탈사이트를 다양한 비율로 합성하여 지지체로 사용하였다.

공침법으로 Mg/Al의 비율이 각각 1:9, 2:8, 3:7, 4:6, 5:5, 6:4가 되도록 하이드로탈사이트를 합성하고 이를 고온에서 소성한 후 질소 산화물 흡장 환원 촉매의 지지체로 사용하였다. 그리고 함침법을 이용해 Pt과 Ba을 담지 하였다. 제조된 촉매들을 500 ℃, 650 ℃, 800 ℃ 에서 소성한 후 BET 표면적, XRD, ICP, FT-IR, Chemisorption, TEM, EDS, TPD, NOx 분석장비를 이용해 각각 촉매의 반응성을 평가하고 특성을 분석하였다.

500 ℃에서 소성한 경우, 기존의 Pt-BaO/Al_2O_3 촉매는 활성온도가 낮고 그 범위가 좁은 데에 반해 하이드로탈사이트를 지지

체로 사용하는 촉매들은 전반적으로 활성 온도가 높고 그 범위가 넓었으며 활성도 우수하였다. 특히, Mg/Al의 비가 2:8인 경우, 최고 활성을 나타내는 온도가 400 ℃로 가장 높았다. 고온에서 소성한 경우, 백금이 소결되므로 Pt-BaO/Al_2O_3 촉매의 활성은 전 온도에서 급격히 감소하였지만 하이드로탈사이트를 지지체로 사용한 촉매는 저온에서의 활성은 감소하지만 고온에서는 NOx 저장 활성이 유지되었다. 그 중 Mg/Al의 비가 4:6인 경우 가장 좋은 활성을 보였다.

본 연구를 통해 하이드로탈사이트를 구성하는 Mg/Al의 비율이 4:6인 경우 질소 산화물 흡장 환원 촉매의 지지체로써 최적화된 비율임을 확인했다. 하이드로탈사이트를 지지체로 사용한 촉매가 기존의 알루미나를 지지체로 사용한 촉매보다 질소 산화물 흡장 능력과 고온에서의 활성이 우수함을 확인하였다. 결론적으로 하이드로탈사이트를 지지체로 사용하는 것이 기존 촉매보다 활성이 우수하며 Pt의 분산도가 개선되고, Pt의 소결이 억제되는 등 열적 내구성이 개선되었기 때문에 알루미나를 대체할 수 있는 대안이 될 것으로 예상한다.

주요어 : 질소 산화물 흡장 환원 촉매, 하이드로탈사이트,

Mg/Al 비율, Pt-BaO, 열적 내구성

학 번 : 2011-23414